Measurement of the nucleon spin structure functions

N. Bianchi
Laboratori Nazionali di Frascati dell'INFN, Frascati, Italy
and
HERMES collaboration

Abstract

The present situation in the knowledge of the spin structure function of the nucleon and the future improvement due to the new HERMES experiment is discussed.

1 Introduction

A few years ago, experimental results from the European Muon Collaboration (EMC) at CERN on the spin structure of the proton challenged the high energy physics community [1]. Quarks seemed to carry a negligible fraction of the nucleon spin, in contradiction with basic ideas about nucleon structure. Several possible explanations were proposed, but the precision of experimental data was not sufficient to provide reliable conclusions. The experimental results had to be confirmed, their kinematics range at lower x and their precision increased. Experimental information on the neutron spin structure, an essential piece of the puzzle, was also missing.

Therefore, a new experimental program was started at CERN by the Spin Muon Collaboration (SMC) [2], at SLAC by the E142 [3] and E143 [4] collaborations and at DESY by the HERMES collaboration [5]. HERMES is a new experiment at HERA (DESY) designed to study the spin structure of the nucleon by deep inelastic scattering of polarised electrons or positrons at 27.5 GeV, off polarised protons and neutrons.

2 Deep inelastic scattering

Deep inelastic scattering is the study of lepton-hadron scattering in the limit of high momentum transfer. For simplicity we can consider the electromagnetic lepton-nucleon scattering: in lowest order QED the scattering process is described by the exchange of a virtual photon.
We denote m the lepton mass, *k (k')* the initial (final) lepton four-momentum, *p (p')* the initial (final) four momentum of the nucleon and $q =$ *k-k'* the four-momentum of the exchanged virtual photon. The following Lorentz invariants are defined in the standard way as [6]:

$$s = (k+p)^2 \qquad Q^2 = -q^2 = -(k-k')^2 > 0$$

$$\nu = p \cdot q / M \qquad W^2 = p'^2 = M^2 + 2M\nu - Q^2$$

where M is the mass of the proton.

The scattering process is then characterised by two invariants Q^2 and ν or, equivalently, by Q^2 and the Bjorken variable $x = Q^2/2\nu$. When $Q^2 \rightarrow \infty$ and $\nu \rightarrow \infty$, the virtual photon interacts with the pointlike constituents of the nucleon. Experimentally, this is observed by the scale invariance predicted by Bjorken, i.e. the deep inelastic cross section depends nolonger on two variables, but only on the dimensionless variable x, the fraction of the proton's momentum carried by the elastically scattered parton, in the high proton momentum limit.

The differential cross section for the One Photon Exchange (OPE) process is given by [7]:

$$\frac{d^2\sigma}{d\Omega dE'} = \frac{\alpha^2}{q^4}\frac{E'}{E}L_{\mu\nu}W^{\mu\nu}$$

where α is the fine structure constant, $L_{\mu\nu}$ and $W^{\mu\nu}$ describe the leptonic and hadronic vertices respectively.

In the case of polarised beam and polarised target the cross section σ can be decomposed into a unpolarised piece σ_0 and a polarised piece $\Delta\sigma$: the unpolarised cross section can be considered as the average of the measurement of both relative orientations and it depends on the spin independent structure functions F_1 and F_2, while the polarised contribution can be written as the difference of the two possible orientations:

$$\Delta\sigma = \frac{1}{2}\left(\frac{\partial^2\sigma^{\uparrow\uparrow}}{\partial x\partial Q^2} - \frac{\partial^2\sigma^{\uparrow\downarrow}}{\partial x\partial Q^2}\right) =$$

$$= \frac{1}{2}\frac{4\pi\alpha^2}{MExQ^2}\left[\left(2 - \frac{Q^2}{2MEx} - \frac{Q^2}{4E^2}\right)g_1(x,Q^2) - \frac{2Mx}{E}g_2(x,Q^2)\right]$$

where g_1, g_2 are the spin dependent structure functions of the nucleon. The structure function g_1 have a simple interpretation in the parton model of Feynman [8]. Defining the parton distributions $q^{\uparrow(\downarrow)}(x)$ and $\bar{q}^{\uparrow(\downarrow)}(x)$ as the probability to find a quark and antiquark, respectively, with momentum fraction x and polarization in the same (opposite) direction as the proton's momentum, the structure function g_1 describe the difference of the spin-weighted momentum distribution of quarks in the nucleon:

$$g_1(x) = \frac{1}{2}\sum_q e_q^2 \Delta q(x)$$

The structure function $g_2(x)$ does'nt have a simple interpretation in the parton model, but it could be considered as a measurement of the difference of longitudinal and transverse spin effect.

Wandzura and Wilczek [9] have shown that in QCD it can be decomposed as:

$$g_2(x,Q^2) = g_2^{WW}(x,Q^2) + \bar{g}_2(x,Q^2)$$

where the "trivial" piece g_2^{WW} is a leading twist contribution and it is completely determined by $g_1(x,Q^2)$:

$$g_2^{WW}(x,Q^2) = -g_1(x,Q^2) + \int_0^1 g_y(y,Q^2)\frac{dy}{y}$$

The term $\bar{g}_2$ is a twist-3 contribution, wich is best understood in an OPE analysis in QCD, where it is sensitive to a quark-gluon correlation function in the nucleon and thus contains unique new physics. In Regge theory, g_2 is shown to fulfill, under certain conditions, the Burkhardt-Cottingham sum rule [10]:

$$\int_0^1 g_2(x,Q^2)dx = 0$$

but this is still controverse [11].

In the Naive Parton Model where each parton carries a fraction x of the nucleon four-momentum $g_2 = 0$. However non zero values of g_2 can be obtained by allowing the quarks to have an intrinsic Fermi motion inside the nucleon: Feynman [8] wrote $g_1(x) + g_2(x) = \frac{1}{2}\sum_q e_q^2 \Delta q_T(x)$ where Δq_T involves number densities of partons with spin perpendicular to that one of the proton.

3 How to measure g_1, g_2

To measure the fraction of the nucleon spin carried by quarks spin, one must therefore freeze both the orientation of the spin of the incoming lepton, and the spin of the target nucleon, so that the lepton and nucleon spins are either parallel or antiparallel to each other. One then measures the cross-section asymmetry, i.e. the difference in the probabilities of scattering leptons from nucleons with spin paralllel or antiparallel to the spin of the incident lepton (these differences are very small $\approx 10^{-3}$).

The polarised piece gives only a small contribution to the cross section and is, in general, experimentally further suppressed by incomplete beam and target polarisations. It is therefore customary to evaluate it from measurement of the cross section asymmetries in which the unpolarised part cancels. When both the beam and the target are longitudinally polarised this asymmetry is:

$$A_{\|} = \frac{\sigma^{\uparrow\downarrow} - \sigma^{\uparrow\uparrow}}{\sigma^{\uparrow\downarrow} + \sigma^{\uparrow\uparrow}} = D[A_1 + \eta A_2]$$

where $\sigma^{\uparrow\downarrow}$ and $\sigma^{\uparrow\uparrow}$ are the cross section for opposite and equal spin directions respectively, D is the depolarization factor of the virtual photon, η is a factor depending on kinematic variables and A_1 and A_2 can be interpreted as virtual-photon asymmetries; for spin 1/2 particles:

$$A_1 = \frac{\sigma_{1/2} - \sigma_{3/2}}{\sigma_{1/2} + \sigma_{3/2}} \qquad A_2 = \frac{2\sigma_{TL}}{\sigma_{1/2} + \sigma_{3/2}}$$

where $\sigma_{1/2(3/2)}$ is the virtual photo-absorbtion cross section when the projection of the total angular momentum fo the photon-nucleon system along the photon direction is 1/2 (3/2) and σ_{TL} is a term arising from the interference between transverse and longitudinal amplitude.

In the same way when the target is transversely polarised the asymmetry is:

$$A_{\perp} = \frac{\sigma^{\uparrow\rightarrow} - \sigma^{\uparrow\leftarrow}}{\sigma^{\uparrow\rightarrow} + \sigma^{\uparrow\leftarrow}} = d[A_2 + \xi A_1]$$

where d, ξ have the same meaning of D, η for transversely polarised targets.

The experimentally measured counting rate asymmetry is related to the cross section asymmetry by $A_{exp} = f_t P_t P_b A_{||}$ where P_b is the beam polarization, P_t the polarization of the target nucleons and f_t the target dilution factor, i.e. the fraction of polarised nucleons in the target material.

The asymmetry A_2 is constrained by the positivity limit $\mid \sqrt{R} \mid$ and this term is small but not negligible at finite values of Q^2: SLAC, EMC and SMC worked with this approximation, so the asimmetry is $A_{||} \cong DA_1$ and the spin structure funtion g_1 is evaluated from the average asymmetry A_1 in each measured x bin using the approximate relation:

$$g_1 \approx \frac{A_1(x) F_2(x, Q^2)}{2x[1 + R(x, Q^2)]}$$

where $F_2(x, Q^2)$ and $R(x, Q^2)$ are taken from unpolarised deep inelastic experiments [12, 13].

Following the same procedure for $A_\perp$ one obtain that a measurement of $A_\perp$ provide direct information on the structure function combination $g_2 + \nu/(2E) g_1$ [14]; in this case the coefficient of g_1 is not negligible and to isolate g_2 one must feed in one's knowledge of g_1 obtained from $A_{||}$ measurement.

From both considerations it appear the importance of combined analysis using $A_{||}$ and $A_\perp$ to extract both g_1 and g_2 and the importance to have $f_t \approx 1$, and P_t, P_b as biggest as possible. The spin structure of the proton can be measured directly using a hydrogen target.

4 Extraction of spin structure function of the neutron

The neutron structure function can be experimentally extracted by two methods. It is firstly derived from the comparison of deuterium and hydrogen targets and secondly from ^3He. The deuteron is a spin-1 target and therefore has three possible orientations $m_I = 1, 0, -1$ of the spin vector relative to the quantisation axis. As the SLAC and CERN experiments cannot measure the $m_I = 0$ component, the nuclear effects in deuterium are accounted for by a global depolarisation factor according to the following equation:

$$A_1^n = \frac{A_1^D}{1 - 1.5\omega_D} \; \frac{\sigma^D}{\sigma^D - \sigma^H} - A_1^H \frac{\sigma^H}{\sigma^D - \sigma^H}$$

where $\omega_D \approx 0.05$ denotes the D-state probability of the deuteron. With HERMES an unambiguous determination of $A_{||}^d$ is possible, because the $m_I = 0$ component can be measured directly as the polarization of the target can be arranged in all substates separately.

The ^3He target could be regarded as good neutron target: the wave-function is almost entirely an S state with two proton having opposite spins, thus most the spin is carried by the neutron. There is some mixing in the wave-function [15, 16] and one estimate $P_n = (87 \pm 2)\%, P_p = (-2.5 \pm 0.3)\%$. Nuclear correction for ^3He are larger than for deuterium, but they are understood with sufficient precision.

HERMES will provide the measurement of the neutron structure function with both target.

The use of different target technologies and different physics assumptions in extraction of the neutron structure functions provides important redundancy in the HERMES measurement.

5 Experimental situation and comparison with precision of the HERMES experiment

HERMES make use of a two novel techniques: a longitudinally polarised electron (positron) beam in a storage ring and an internal polarised gas target.

The beam polarisation is naturally in the transverse direction due to the Sokolov-Ternov effect [17], while spin rotators are used to rotate the spin into the longitudinal direction [18]. The maximum polarisation achieved is 70%, and the polarisation build-up time is significantly short (≈ 35 min). The mean beam polarization is generally $\geq 50\%$.

The internal gas targets have the important advantage of being pure atomic species, so they can be polarised to a high degree without or with only small dilution by unpolarised nuclei; they also allow for rapid polarisation reversal and are therefore an ideal choice to minimise systematic errors wich originate in time dependent intrumental effects. The targets are very thin ($\approx 10^{-10}$ radiation lengths), with no windows, so if the electron beam is suitably well focused, scattering occurs only from the polarised target atoms. The polarization for the H/D targets is $\geq 80\%$ and that one for ^3He is $\geq 50\%$.

The luminosity for a 30 mA circulating electron beam is $1.8 \div 50 \cdot 10^{31}$ nucleons $cm^{-2}s^{-1}$.

The HERMES detector is installed in the interaction region of HERA East Hall. As shown in the fig. 1 the detector [5] consists mainly of a spectrometer magnet, tracking device and a PID detector and is able to measure the scattered electron and the total hadronic final state in a wide kinematic range and with a good angular and momentum resolution. The microstrip gas counters and front drift chambers provide vertex reconstruction to the target, as well the scattering angle and track definition into the spectrometer; the proportional chambers inside the magnet help to resolve multitrack ambiguities, while the back drift chambers complete the momentum measurement. The second part of the spectrometer is an electromagnetic calorimeter, consisting of a preshower counter (11 mm lead sheet and a scintillator) and of a wall of lead glass blocks, used as trigger device for measuring the energy of electrons and photons and for $\pi - e$ separation; the electron identification is improved also by a transition radiation detector, while a threshold Čerenkov counter allows the pion-kaon separation in the momentum range below 15.8 GeV. The kinematical region covered by the experiment is:

$$0.02 < x < 0.8 \qquad Q^2 > 1(GeV/c)^2 \qquad W > 2GeV$$

$$y > 0.85 \qquad 40\ mrad < \theta < 220\ mrad$$

being θ the scattering angle.

Starting from these consideration the aim of HERMES is to measure the spin dependent structure of nucleons as completely and as precisely as possible.

It is possible to compare the precision of HERMES with that one from SLAC and SMC.

The surprising results observed by the EMC collaboration in 1988 [1] are now confirmed by the new more precise proton data of the SMC [2] and E143 collaborations [4]. In fig. 2 is shown the world data on the spin structure of the proton $g_1^p(x)$; the bands below the points show the systematic errors of the measurements. From the plot is possible to see that the data sets are compatible within their errors and E143 has the most precise measurement until now. In the top part of the figure is shown the anticipated precision of the HERMES data from one *standard run* ($\approx$ 9 weeks with normal condition of beam and target polarization - 0.5 and 0.8 respectively -) normal target density ($\approx 10^{14}$) and normal life time of the beam (around 8 hours with I $\approx 35mA$) [19]. In this case the predicted precision of E143 and one HERMES *standard run* are comparable; if the running time will be more than 9 weeks the size of HERMES errors bars will decrease.

In fig. 3 is shown the SLAC data on the spin structure function of the neutron $g_1^n(x)$; the precision of $g_1^n(x)$ is still very poor. As before, in the top part of the figure are indicated the anticipated precision for the ^3He and $D-H$ measurements of HERMES for one *standard run*. The experimental situation of g_2 is still very open. First data from E142 [3] indicate that A_2^n is limited by $\mid A_2^n(x) \mid < 0.25$ and SMC data [20] indicate that A_2^p is small compared to the positivity limit $\sqrt{R}$. The results for $g_2(x)$ are shown in fig. 4, where it is possible to see that $g_2(x)$ is know with only marginal precision because the measurement of $g_2(x)$ requires a high statistic experiment as it is derived from the difference of the longitudinal and transverse asymmetries; HERMES will be able to determine it much more precisely as shown in the top part of the figure.

6 Bjorken and Ellis-Jaffe sum rules

Like in the unpolarised scattering, no precise theoretical prediction exists for the x dependence of spin-dependent structure functions; there are, however, theoretical predictions for the momenta:

$$\Gamma_1^{p(n)} = \int_0^1 g_1^{p(n)}(x)dx$$

The Bjorken sum rule relates the difference between proton and neutron spin structure to the axial charges g_A and g_V measured in Gamow-Teller nuclear β decay [21]. The sum rule can be derived in QCD in the limit $Q^2 \rightarrow \infty$; at finite values of Q^2 [22]:

$$\Gamma_1^p(Q^2) - \Gamma_1^n(Q^2) = \frac{1}{6} \mid \frac{g_A}{g_V} \mid \Big[1 - \frac{\alpha_s(Q^2)}{\pi} - ...\Big]$$

where there are computations of QCD corrections up to $O(\alpha_s^3)$ [23] and an estimation for the $O(\alpha_s^4)$ corrections [24].

Experimentally, combining all the available data at $Q^2 = 5\ GeV^2$ the result is: $\Gamma_1^p - \Gamma_1^n = 0.162 \pm 0.014$, to be compared to a predicted $\Gamma_1^p - \Gamma_1^n = 0.182 \pm 0.0005$. Thi mean that the Bjorken sum rule is confirmed at the one sigma level.

The dependence of the Bjorken integral on QCD correction can be used to extract the value of strong coupling constant α_s [25].

Separated sum rules for the proton and neutron were derived by Ellis and Jaffe [26], using the Constituent Quark Model and assuming that there was no contribution to the spin structure from virtual strange-antistrange quarks in the "sea" ($\Delta s = 0$):

$$\Gamma_1^{p(n)} = \int_0^1 g_1^{p(n)}(x)dx = \frac{1}{12}\left(\pm a_3 + \frac{a_8}{3}\right) + \frac{1}{9}a_0 + QCD_{corrections}$$

where a_0, a_3, a_8 are the weak axial-vector coupling constants.

In flavour $SU(3)$ symmetry a_3 and a_8 are related to the symmetric and antysimmetric weak $SU(3)_f$ couplings F and D of the baryon octet:

$$a_3 = \Delta u - \Delta d = \mid \frac{g_A}{g_V} \mid = F + D$$

$$a_8 = \Delta u + \Delta d - 2\Delta s = 3F - D$$

$$a_0 = \Delta\Sigma = \Delta u + \Delta d + \Delta s$$

The comparison between the E.J. integral with combined CERN and SLAC data and the theoretical value with QCD corrections and for $Q^2 \approx 10\ GeV^2$ is [27]:

$$\Gamma_1^p = (0.176 \pm 0.006)_{theor} = (0.126 \pm 0.018)_{EMC/SLAC}$$

The new data from SLAC [3, 4] and SMC [2] confirm the violation of the Ellis Jaffe sum rule at the 2.5 σ level. This violation caused the so-called *spin crisis*, because the total spin carried by quarks $\Delta\Sigma$ is different from the theory and from the experiments:

$$\Delta\Sigma_{E.J.} = \Delta u + \Delta d \cong 0.6$$

$$\Delta\Sigma_{SLAC-CERN} \approx 0.2 \div 0.3$$

with the conclusion that only a small part of the proton's spin is due to the intrinsic spin of the quarks. One of the possible solution is that the momentum-transfer dependence of each quark spin fraction is associated with the gluon spin distribution. The up-quark contribution Δu, for example, is given by:

$$\Delta u(Q^2) = \Delta u_0 - \frac{\alpha_s}{2\pi}\Delta G(Q^2)$$

where Δu_0 is the Q^2 independent component of the up-quark spin fraction.

7 Conclusions

The spin structure of the nucleon is now better understood than a few years ago, when the EMC polarized data were published. A considerable theoretical effort has been done and major progress has been achieved, but the existing data are still not sufficient to explain the spin structure of the nucleon: many new theoretical models have been developed over the last years and more complete and precise experimental data are needed. The HERMES experiment has been designed to cope with these requirements in two ways: it will measure with high systematic and statistical precision the spin structure functions of proton and neutron by studying double-polarised, inclusive deep inelastic scattering. Secondly by measuring the seminclusive channel (the real strength of this experiment, but not discussed here) HERMES will be able to disentangle the spin contribution from up, down and strange quarks and to some extend also the contribution from gluons and from angular momentum of the quarks, with good chances to solve a large fraction of the spin puzzle.

HERMES started measurements in summer 1995 with ^3He target; in 1996 it is planned to interchange between hydrogen and ^3He target and to disentangle spin distribution of different quark flavours.

References

[1] EMC, J. Ashman et al., Phys. Lett. B206 (1988) 364;
EMC, J. Ashman et al., Nucl. Phys. B328 (1989) 1.

[2] SMC, D. Adams et al., Phys. Lett. B329 (1994) 399.

[3] E142, P.L. Anthony et al. Phys. Rev. Lett. 71 (1993) 959.

[4] E143, K. Abe et al., Phys. Rev. Lett. 74 (1995) 346.

[5] HERMES Collaboration, Technical Design Report, DESY - PRC 93/06 (1993).

[6] R.G. Roberts, The structure of the proton (Cambridge University Press, 1990).

[7] F.E. Close, An introduction to quarks and partons (New York Academic, 1979);
E. Leader-E. Predazzi, An introduction to gauge theories and the new physics (Cambridge University Press, 1982).

[8] R.P. Feynman, Phys. Rev. Lett. 23, 1415;
R.P. Feynman, Photon-hadron interactions (B. Cummings-New York, 1972).

[9] S. Wandzura-F. Wilczek, Phys. Lett. B72 (1977) 195.

[10] H. Burkhardt-W.N. Cottingham, Ann. Phys. (N.Y.) 56 (1970) 453;
R.L. Jaffe, Comments Nucl. Part. Phys. 19 (1990) 239.

[11] G.Altarelli et al., Phys. Lett. B334 (1994) 187.

[12] NMC, P. Amaudruz et al., Phys. Lett. B295 (1992) 159.

[13] L.W. Whitlow et al., Phys. Lett. B250 (1990) 193.

[14] M. Anselmino et al., CERN-TH 7216/94.

[15] R.M. Woloshyn, Nucl. Phys. A496 (1989) 749.

[16] C. Ciofi degli Atti et al., Phys. Rev. C48 (1993) R968 .

[17] A.A. Sokolov-I.M. Ternov, Sov. Phys. Dokklady 8 (1964) 1203.

[18] D.P. Barber et al., Phys. Lett. B343 (1995) 436.

[19] M. Dueren, DESY-HERMES 95-02.

[20] SMC, D. Adams et al., Phys. Lett. B336 (1994) 119.

[21] J.D. Bjorken, Phys. Rev. 148 (1966);
J.D. Bjorken, Phys. Rev. D1 (1970) 465;
J.D. Bjorken, Phys. Rev. D1 (1970) 1376.

[22] J. Kodaira et al., Phys. Rev. D20 (1979) 627;
J. Kodaira et al., Nucl. Phys. B159 (1979) 99;
J. Kodaira et al., Nucl. Phys. B165 (1980) 129.

[23] S.A. Larin-J.A.M. Vermaseren, Phys. Lett. 66 (1991) 862;
S.A. Larin-J.A.M. Vermaseren, Phys. Lett. B259 (1991) 345.

[24] A.L. Kataev-V. Starshenko, CERN TH-7198/94.

[25] S.A. Larin, Phys. Lett. B334 (1994) 399;
J.Ellis-M.Karliner, Phys. Lett. B341 (1995) 397.

[26] J. Ellis-R.L. Jaffe, Phys. Rev. D9 (1974) 1444;
J. Ellis-R.L. Jaffe, Phys. Rev. D10 (1974) 1669.

[27] R.L. Jaffe, Phys. Today (sep. 1995), 24

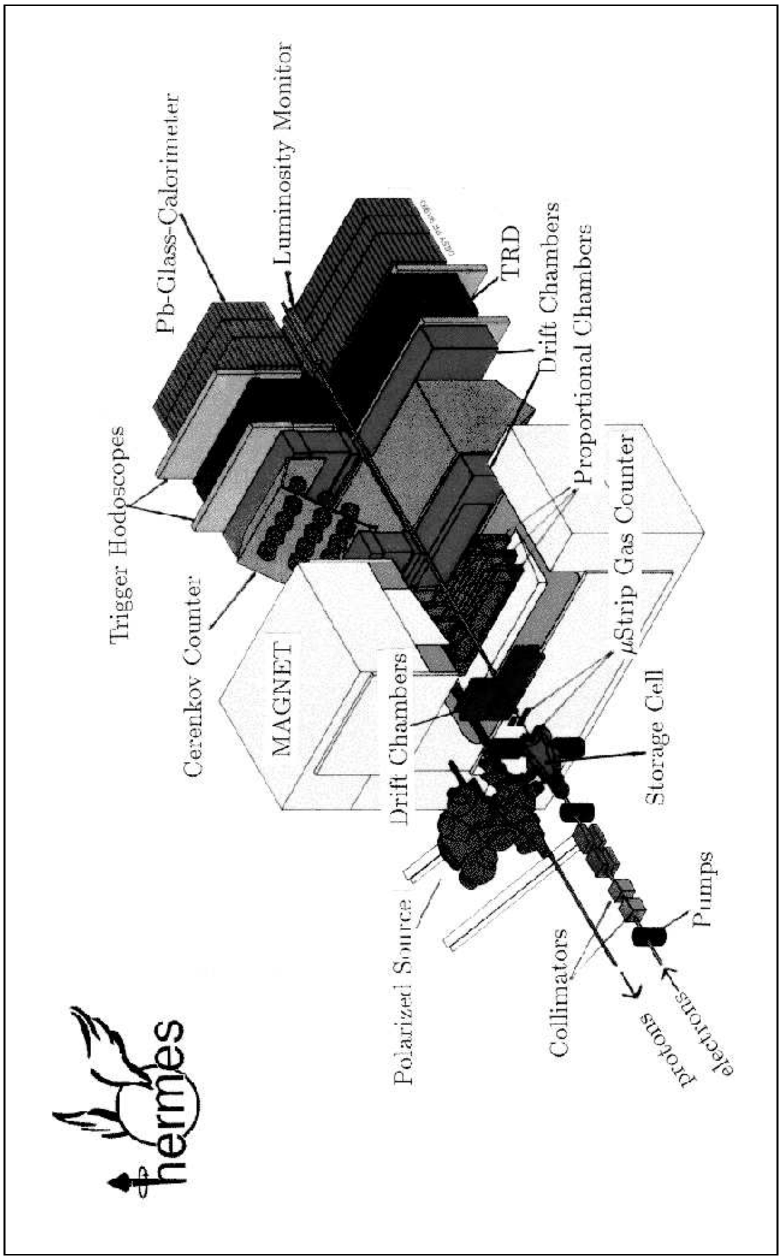

Figure 1: Schematic view of the spectrometer.

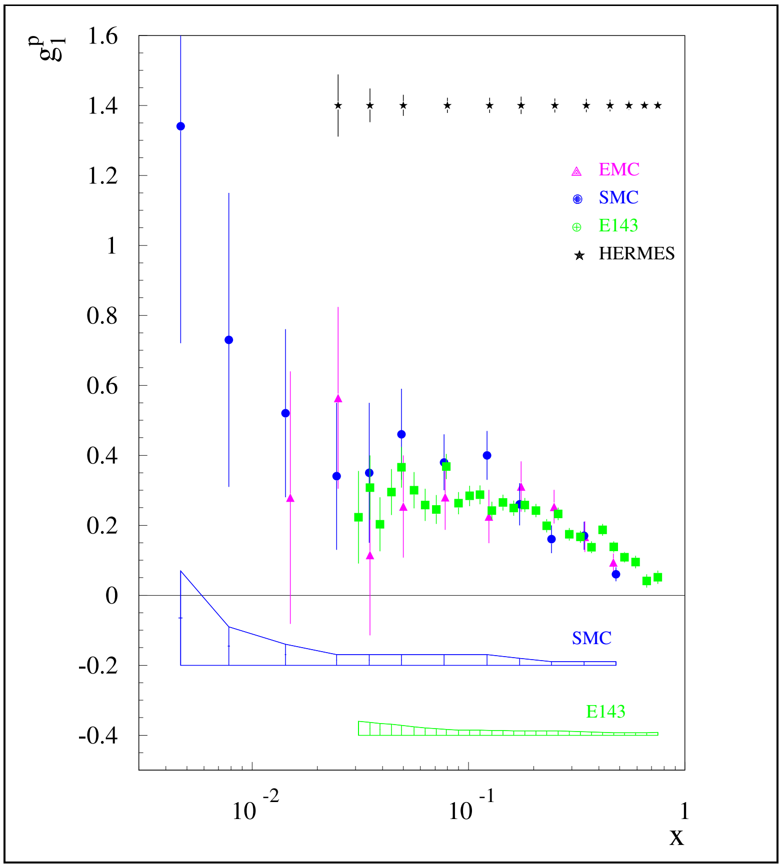

Figure 2: The world data on the spin structure funtion $g_1^p(x)$ of the proton. The bars below the figures indicate the systematic errors; the anticipated precision of HERMES experiment is indicated in the error bars at the top part of the figure.

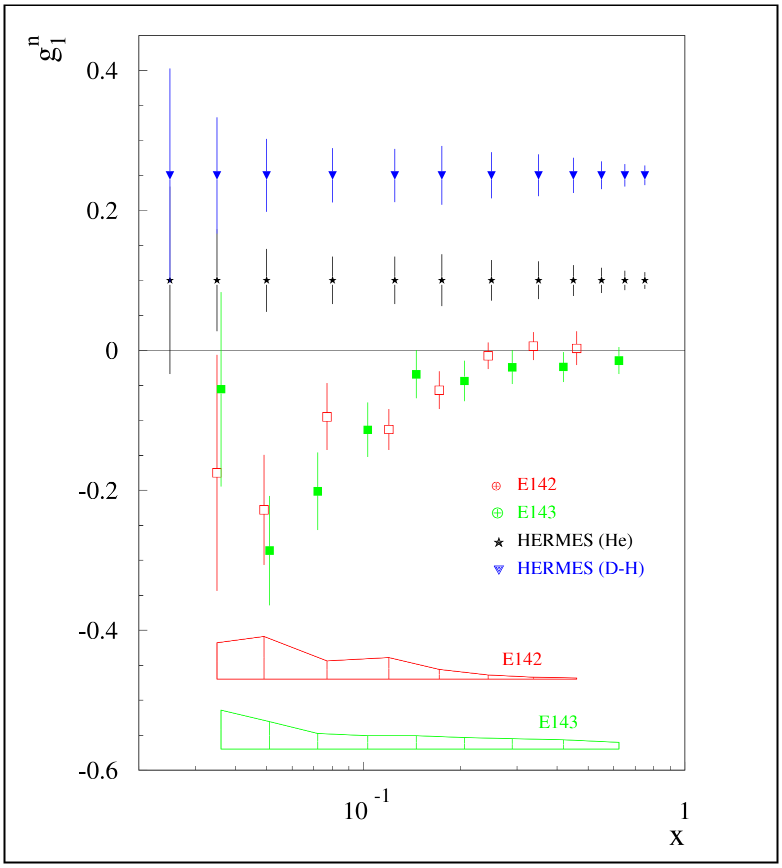

Figure 3: The world data on the spin structure funtion $g_1^n(x)$ of the neutron. As before the precision of HERMES experiment for one standard run is indicated in the error bars at the top part of the figure.

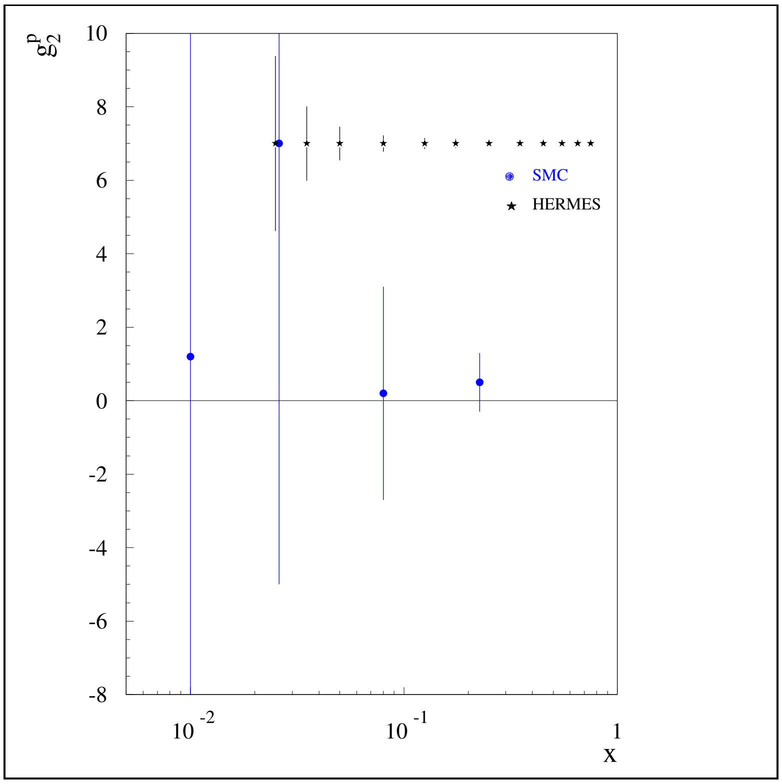

Figure 4: First data on the second spin structure function $g_2^p(x)$ as taken by SMC. The precision for HERMES standard run is indicated in the top part of the figure.